



## Dissolution of kraft lignin in alkaline solutions

Elodie Melro<sup>a,\*</sup>, Alexandra Filipe<sup>b</sup>, Dora Sousa<sup>c</sup>, Artur J.M. Valente<sup>a</sup>, Anabela Romano<sup>c</sup>,  
Filipe E. Antunes<sup>a</sup>, Bruno Medronho<sup>c,d</sup>

<sup>a</sup> CQC, Department of Chemistry, University of Coimbra, Rua Larga, 3004-535 Coimbra, Portugal

<sup>b</sup> CIEPQPF, Department of Chemical Engineering, University of Coimbra, Pólo II – R. Silvio Lima, 3030-790 Coimbra, Portugal

<sup>c</sup> MED – Mediterranean Institute for Agriculture, Environment and Development, University of Algarve, Faculty of Sciences and Technology, Campus de Gambelas, Ed. 8, 8005-139 Faro, Portugal

<sup>d</sup> FSCN, Surface and Colloid Engineering, Mid Sweden University, SE-851 70 Sundsvall, Sweden

### ARTICLE INFO

#### Article history:

Received 22 November 2019

Received in revised form 14 January 2020

Accepted 16 January 2020

Available online 16 January 2020

#### Keywords:

Alkaline solvents

Dissolution

Kraft lignin

### ABSTRACT

Lignins are among the most abundant renewable resources on the planet. However, their application is limited by the lack of efficient dissolution and extraction methodologies. In this work, a systematic and quantitative analysis of the dissolution efficiency of different alkaline-based aqueous systems (i.e. lithium hydroxide, LiOH; sodium hydroxide, NaOH; potassium hydroxide, KOH; cuprammonium hydroxide, CuAOH; tetrapropylammonium hydroxide, TPAOH and tetrabutylammonium hydroxide, TBAOH) is reported, for the first time, for kraft lignin. Phase maps were determined for all systems and lignin solubility was found to decrease in the following order: LiOH > NaOH > KOH > CuAOH > TPAOH > TBAOH, thus suggesting that the size of the cation plays an important role on its solubility. The  $\pi^*$  parameter has an opposite trend to the solubility, supporting the idea that cations of smaller size favor lignin solubility. Dissolution was observed to increase exponentially above pH 9–10 being the LiOH system the most efficient. The soluble and insoluble fractions of lignin in 0.1 M NaOH were collected and analyzed by several techniques. Overall, data suggests a greater amount of simple aromatic compounds, preferentially containing sulfur, in the soluble fraction while the insoluble fraction is very similar to the native kraft lignin.

© 2020 Elsevier B.V. All rights reserved.

## 1. Introduction

Lignin is a highly branched aromatic polymer, plentifully available in nature, which is believed to bind cellulose and hemicellulose, via strong hydrogen bonding and ester linkages, in the cell walls of vascular plants [1–4]. Lignin is synthesized from random polymerization of three main phenylpropane monomers: coumaryl, coniferyl and sinapyl alcohols [5]. The phenylpropanoid units are linked to each other by various types of ether and carbon-carbon bonds [6] thus rendering a highly complex and heterogeneous three-dimensional structure [7,8].

Lignin is commonly regarded as a waste in lignocellulosic biomass biorefinery despite being a large carbon and energy reserve with high potential as an aromatic feedstock commodity [9]. For instance, lignin can work as a natural broad-spectrum UV blocker due to its functional groups [10]. Lignin versatility is also patent in its use as, for instance, an antioxidant and antibacterial agent [11], excipient for controlled drug release [12,13] or even as building block in the development of different value added materials, such as carbon fibres [14–16].

Despite its potential, its use is still negligible mainly due to scarce separation techniques available which, in most of the cases, result in

low extraction yields, extensive degradation or even undesired chemical modifications.

Lignin can be extracted from pulping chemical processes, resulting in technical lignins such as kraft, liginosulfonate, soda and organosolv. The kraft process is considered the dominant method to remove lignin during cellulose extraction and purification, with ca. 85% of the total world lignin production being obtained by this method [17]. It employs high pHs and considerable amounts of aqueous sodium hydroxide and sodium sulfide [18], resulting in a rather hydrophobic material, kraft lignin [19]. Apart from the kraft pulping of wood, the cellulosic bioethanol production has been estimated to contribute with ca. 60 million tons/year of lignin [20].

Due to the high structural and chemical heterogeneity of lignin and extraction methods, dissolution systems must be adapted [21]. The lignin dissolution, as an often required first step for several production processes and applications, is still rather complex. Nevertheless, a wide variety of solvents for lignin have already been developed and, among them, organic based, ionic liquids and deep eutectic solvents are particularly relevant [22]. The solvent selection may also affect the final application. For example, in some electrochemical applications, the activation of lignin is a crucial step in order to increase the quantity of carbonyl groups. This can be achieved by dissolving lignin in ionic liquids [23–25]. A strong aqueous alkaline solvent is a preferential system

\* Corresponding author.

E-mail address: [elodie.melro@uc.pt](mailto:elodie.melro@uc.pt) (E. Melro).

cited in the literature for dissolving kraft lignin but, surprisingly, the solubility of lignin in these systems has not been properly described. The information is scarce and it is only known that, in alkaline solution, the kraft lignin components adopt a polyanionic character [26], where the solubility is influenced by the pH [27]. The complete dissolution is suggested to be reached at complete ionization of all its phenolic hydroxyls [28]. Besides that, the components of kraft lignin have an apparent expanded random coil conformation in aqueous alkaline solution [29].

It is clear that alkaline-based aqueous solvents are of remarkable academic and industrial importance. However, literature reporting lignin dissolution in this class of solvents is clearly lacking. Therefore, in this work we address this problem and present a comprehensive study where several alkaline solutions, namely, lithium, sodium, potassium, cuprammonium, tetrabutylammonium and tetrapropylammonium hydroxides are used to systematically dissolve kraft lignin. The correlation of lignin solubility with the Kamlet-Taft solvatochromic parameters ( $\pi^*$  and  $\beta$ ) is further analyzed. In addition, after mapping lignin solubility, its soluble and insoluble fractions are analyzed by infrared spectroscopy, elemental analysis, thermogravimetry and gas chromatography coupled with mass spectroscopy.

## 2. Materials and methods

### 2.1. Materials

Kraft lignin, dichloromethane anhydrous (DCM), tetrapropylammonium hydroxide (TPAOH) solution 1.0 M in water, carbon tetrachloride (CCl<sub>4</sub>) anhydrous, benzene anhydrous, hexane analytical standard, 1,2-dichloroethane (DCE) anhydrous and dimethylformamide (DMF) anhydrous were purchased from Sigma-Aldrich. Lithium hydroxide (LiOH) monohydrate and tetrabutylammonium hydroxide (TBAOH) solution, 40 wt% in water were obtained from Fluka Chemie AG. Sodium hydroxide (NaOH) and potassium hydroxide (KOH) were purchased from José Manuel Gomes dos Santos, Lda., (Porto, Portugal) while cuprammonium hydroxide (CuAOH) was obtained from BDH. The 4-nitroanisole (4NA) and 4-nitrophenol (4NP) were acquired from Dagma. All the chemicals were used as received.

### 2.2. Solubility of lignin and phase maps

Dispersions of kraft lignin (20 wt%) were mixed with vigorous magnetic stirring for 24 h at room temperature. After centrifugation for 1 h at 14000 rpm, the supernatant was removed and diluted with 1 wt% NaOH to determine the total dissolved lignin content. The concentration of lignin was measured on a UV-Vis spectrophotometer (Shimadzu UV-2450) at 288 nm. For the phase map determination, different lignin and solvent amounts were mixed and vigorously stirred with a magnetic stirrer for 24 h at room temperature. Samples were left to equilibrate and inspected over time by naked eye and under optical light microscopy.

#### 2.2.1. Optical light microscopy

A Linkam LTS 120 microscope equipped with a Q imaging (Qicam) Fast 1394 camera was used to observe the lignin dissolution state in the different aqueous-based alkaline solutions. Samples were illuminated with linearly polarized light and examined through a crossed polarizer. Images were analyzed using the Qcapture software.

### 2.3. Solvatochromic Kamlet-Taft measurements

The solvatochromic probes 4-nitroanisole (4NA) and 4-nitrophenol (4NP) were used to estimate the Kamlet-Taft parameters  $\beta$  (polarizability/dipolar effects) and  $\pi^*$  (hydrogen-bond acceptor ability or basicity). Stock solutions of the dyes in DCM were

prepared with a concentration of 4 mM. The dye stock solution was added to the solvents to a final concentration of 0.1 mM, which enables to obtain the absorbance values within the required measurable range. The DCM was removed by evaporation at room temperature. The absorption spectra of the solvatochromic probes was recorded from 250 nm to 500 nm in a quartz cell with a 10 mm path length, using a Shimadzu UV/Vis spectrometer UV-1700 at 1 nm stepwise, and the wavelength of maximum absorption ( $\nu_{max}$ ) as determined for each probe.

#### 2.3.1. Determination of the $\beta$ and $\pi^*$ parameters

The methodology adopted to estimate  $\beta$  is similar to that described by Eychens et al. [30]. The linear equation was determined using non-hydrogen bond accepting solvents (CCl<sub>4</sub>, benzene, hexane, DCM and DCE) and the  $\beta$  parameter was calculated for the solvents of interest in relation to DMF (a strongly hydrogen accepting solvent), by applying the equation:

$$\beta = \frac{1.070 \times \nu_{max}(4NA) - \nu_{max}(4NF) - 1.477}{1.598} \quad (1)$$

The  $\pi^*$  parameter was determined according to Kamlet et al. [31], using the equation:

$$\pi^* = \frac{(\nu_{max}(4NA) - \nu_0)}{s} \quad (2)$$

where  $\nu_0$  and  $s$  are parameters taken from the literature, 34.12 kK and  $-2.343$  kK, respectively, that were obtained from multiple correlation equations that set  $\pi^*$  at zero for cyclohexane and unity for dimethyl sulfoxide [32].

### 2.4. Rheometry

The rheological measurements were carried out on a HAAKE MARS III (Thermo Fisher Scientific) using a plate-plate geometry (35 mm, 0.2 mm gap). A peltier unit was used to ensure strict temperature control, which was set to  $20.0 \pm 0.1$  °C. The storage modulus ( $G'$ ), the loss modulus ( $G''$ ) and the complex viscosity modulus ( $\eta^*$ ) were accessed by performing dynamic oscillatory tests from 100 to 0.01 Hz, at a constant stress of 10 Pa.

### 2.5. Fourier transform infrared spectroscopy (FTIR)

Infrared spectra were recorded with a Thermo Nicolet 380 FT-IR apparatus (Thermo Scientific) equipped with Smart Orbit Diamond ATR system. FTIR spectral analysis was performed within the wave number range of 4000–400 cm<sup>-1</sup>. A total of 68 scans were run to collect each spectrum at a resolution of 2 cm<sup>-1</sup> in the absorbance mode. Background spectra were collected before every analysis. All the samples were freeze-dried before analysis.

### 2.6. Elemental analyzes

Elemental analyzes (C, H, S) were carried out on an Elementar Vario Micro Cube analyzer.

### 2.7. Thermogravimetric analysis (TGA)

Thermograms were measured using a thermogravimetric analyzer, TG 209 F Tarsus (Netzsch Instruments). Typically, 3 mg of lyophilized material was weighed and heated from 25 to 1000 °C at a heating rate of 10 °C · min<sup>-1</sup> under N<sub>2</sub> atmosphere (flow rate of 50 mL · min<sup>-1</sup>).

**Table 1**  
Kraft lignin solubility in different alkaline solutions, at 25.0 °C.

Alkaline solution concentration (M)	Lignin solubility (wt%)					
	LiOH	NaOH	KOH	CuAOH	TPAOH	TBAOH
0.1	4.29 ± 0.03	3.58 ± 0.05	3.28 ± 0.08	2.70 ± 0.06	0.57 ± 0.00	0.40 ± 0.00
0.2	9.73 ± 0.06	8.50 ± 0.06	6.27 ± 0.08	5.65 ± 0.01	0.89 ± 0.01	0.48 ± 0.01

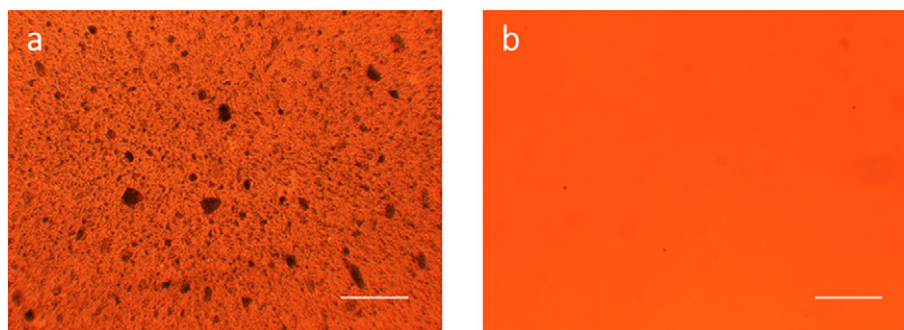


**Fig. 1.** Polarized light micrographs of 30 wt% kraft lignin dissolved in (a) 2 wt% and (b) 4 wt% NaOH at room temperature. The scale bars represent 100  $\mu\text{m}$ .

### 2.8. Gas chromatography–mass spectroscopy (GC–MS)

Chromatograms were obtained in a 7820A GC system (Agilent Technologies), equipped with a mass spectrometer MSD 5975 (Agilent Technologies) with a column of  $30\text{ m} \times 250\ \mu\text{m} \times 0.25\ \mu\text{m}$  HPS-MS. Helium was used as carrier gas at a flow rate of  $1.33\ \text{mL min}^{-1}$ . The injector, interface, quadrupole and ion source temperatures were 250, 300, 150, and 230 °C respectively. The temperature program was set from 70 to 250 °C ( $15\ \text{°C} \cdot \text{min}^{-1}$ , hold time: 10 min) and from 250 to 290 °C ( $5\ \text{°C} \cdot \text{min}^{-1}$ , hold time: 2 min). The samples were previously dispersed in methanol.

## 3. Results and discussion

### 3.1. Effect of cation on solubility of kraft lignin

The solubility of lignin in the different alkaline aqueous solutions was evaluated and found to evolve in the following order:  $\text{LiOH} > \text{NaOH} > \text{KOH} > \text{CuAOH} > \text{TPAOH} > \text{TBAOH}$  (Table 1) regardless the solvent concentration. This result suggests that the cation plays an important role in lignin dissolution since the larger the ionic radius of the cation the poorer the dissolution. Comparing to other relevant biopolymers, the lignin dissolution trend for the hydroxides with alkali metal cations is similar to cellulose (i.e. LiOH is the most efficient

solvent) while in the chitin case it is the reverse (i.e. KOH is the most efficient solvent) [33]. We also note that while the bulky amphiphilic cation tetrabutylammonium,  $\text{TBA}^+$ , is important in cellulose dissolution [34], apparently it is not benefic in the lignin case since all the systems containing these bulky cations present a modest dissolution performance. It is also interesting to observe that in the cases of chitin and cellulose, subzero temperatures are required for dissolution in alkali-based systems, while lignin is observed to dissolve at 25 °C. Another aspect worth mentioning regarding the differences between the dissolution of cellulose and lignin is the fact that cellulose has an optimal NaOH concentration range for a complete dissolution, i.e., above or below this range the dissolution is not achieved [35]. On the other hand, in the lignin case, the solubility increases continuously with the concentration of hydroxide (Fig. 1). Fig. 1a shows non-dissolved lignin particles, while Fig. 1b shows a fully dissolved system with no perceptible particles in solution.

#### 3.1.1. Kamlet-Taft parameters

The empirical polarity of the solvents was evaluated by the Kamlet-Taft parameters, namely in terms of  $\pi^*$  (polarizability/dipolar effects) and  $\beta$  (hydrogen-bond acceptor ability or basicity) scales. The solvatochromic parameter  $\pi^*$  is represented in Fig. 2 and follows the order  $\text{LiOH} < \text{NaOH} < \text{KOH} < \text{TBAOH}$ . This tendency shows that low polarizability favors lignin solubility. The decrease of  $\pi^*$  with the decrease of cation size is a consequence of the expected increase in the charge density [36]. The importance of the hydrogen-bond basicity of the solvent system has been recognized for the dissolution of cellulose [37]. However, lignin does not show the same tendency. The TBAOH system presents the higher  $\beta$  value but the lignin solubility is very low in this solvent (Fig. 2).

#### 3.1.2. Phase maps

In order to better evaluate the efficiency of dissolution of the different systems, the range of concentrations of lignin and alkaline solvent has been extended and the areas of complete and incomplete dissolution are mapped in Fig. 3. In the LiOH system, it is possible to solubilize ca. 30 wt% of lignin using 2 wt% (0.84 M) of LiOH. Despite this hydroxide has proven to be the most effective, its poor solubility in water represents a serious limitation to be considered when dissolving higher amounts of lignin. Using NaOH and KOH, it is possible to dissolve ca. 40 wt% of lignin, with 6 wt% (1.5 M) and

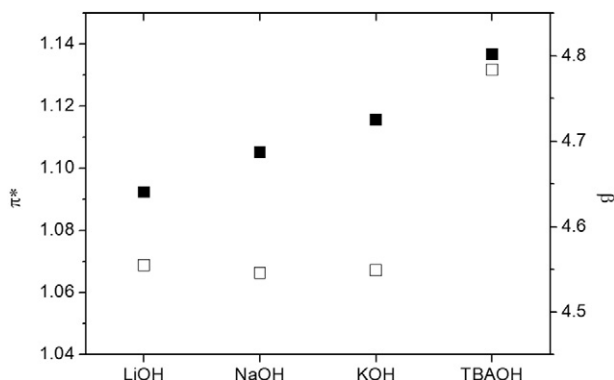


**Fig. 2.** Solvatochromic parameters,  $\pi^*$  (full symbols) and  $\beta$  (empty symbols), for 0.2 M LiOH, NaOH, KOH and TBAOH solvents determined at room temperature.

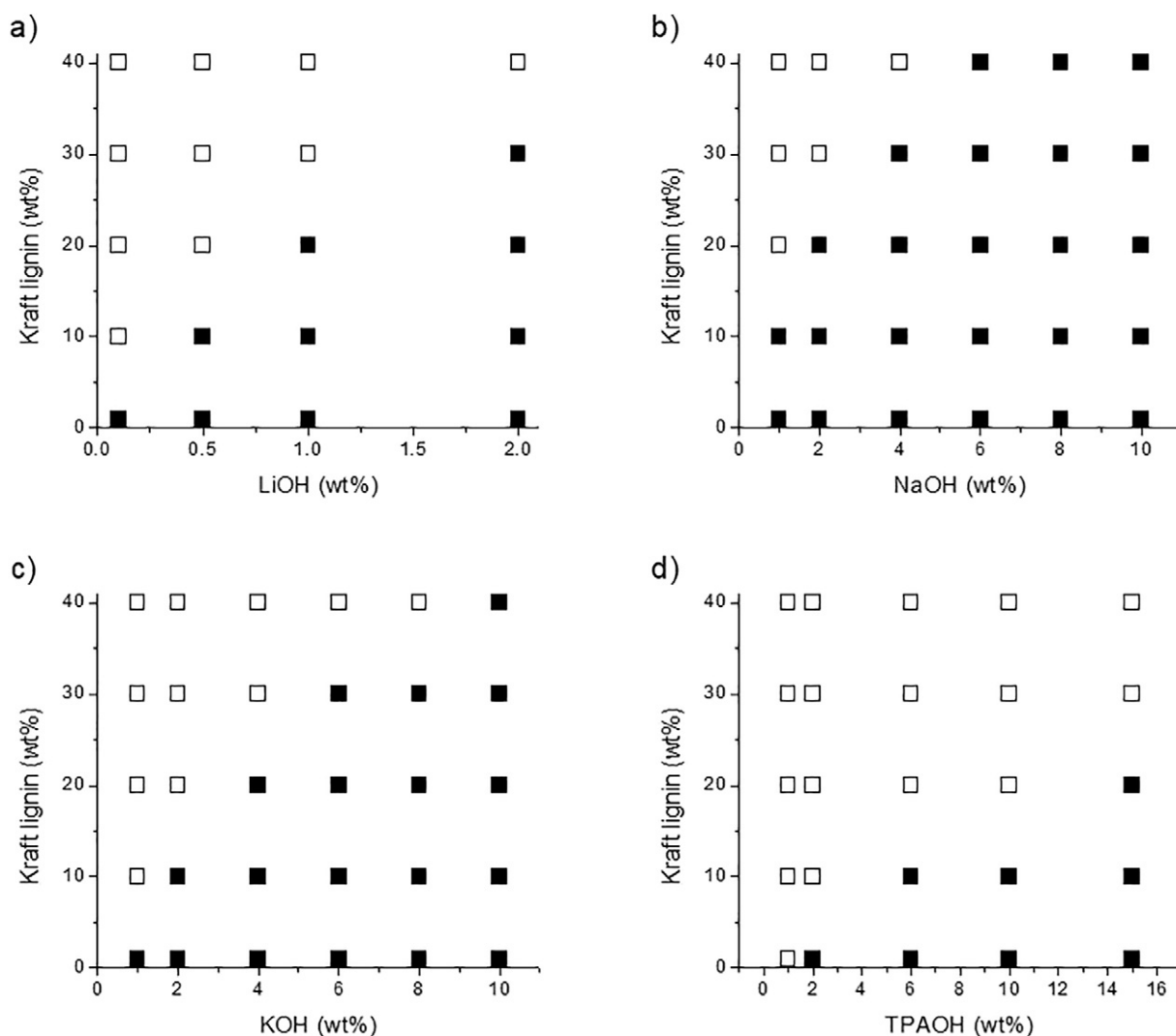


**Fig. 3.** Phase maps representing the complete (full symbols) and incomplete (empty symbols) dissolution of kraft lignin in (a) LiOH (b) NaOH (c) KOH and (d) TPAOH aqueous based solvent systems at room temperature.

10 wt% (1.8 M) of aqueous hydroxides, respectively. In the case of TPAOH, with 15 wt% (0.74 M) of this hydroxide complete dissolution was verified only until ca. 20 wt% of lignin.

### 3.1.3. Rheology

The effect of NaOH concentration in the rheological parameters was evaluated using 10, 20, 30 and 40 wt% of kraft lignin and the results are depicted in Fig. 4. As expected, the viscosity of lignin solutions increases with increasing polymer concentration. For high concentrations of lignin, in the range of complete dissolution, the increase of the hydroxide concentration induces a lower viscosity of the solution. This can be due to charge screening effects, i.e., when the concentration of sodium ion increases, the electrostatic repulsive forces within the polymers are screened and the chains collapse, causing a decrease of the hydrodynamic radius and thus reducing the degree of chain entanglement [38].

### 3.1.4. Effect of pH in kraft lignin solubility

Literature suggests that the solubility of lignin in alkaline solution is a function of pH [28,39,40]. In order to evaluate if the dissolution behavior was exclusively pH dependent or if the type of hydroxide has any effect on it, the solubility of 1 wt% lignin as a function of pH was analyzed using LiOH, NaOH and KOH. From the data presented in Fig. 5, it is possible to observe that below pH 10, pH has a minor effect on lignin solubility. On the other hand, above pH 10, the solubility efficiency increases

exponentially following the same trend as described above, i.e. for the same pH, the lignin solubility order is: LiOH > NaOH > KOH. In practice, this means that a complete dissolution occurs at a slightly lower pH using LiOH.

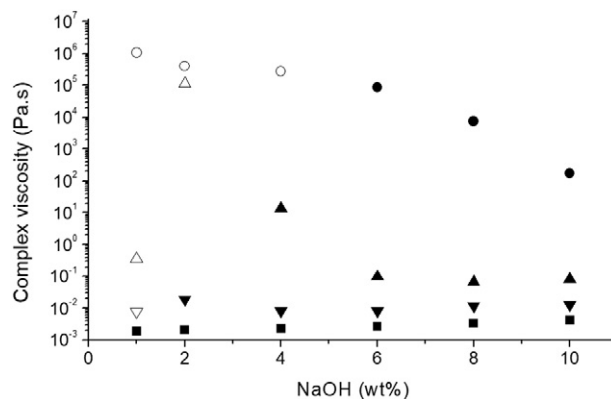


**Fig. 4.** Complex viscosity ( $\eta^*$ ) at 10 Pa, 0.1 Hz and 20 °C, for 10 (■), 20 (▼), 30 (▲) and 40 (●) wt% kraft lignin dispersed in sodium hydroxide with different concentrations. The full symbols represent the complete dissolution cases.

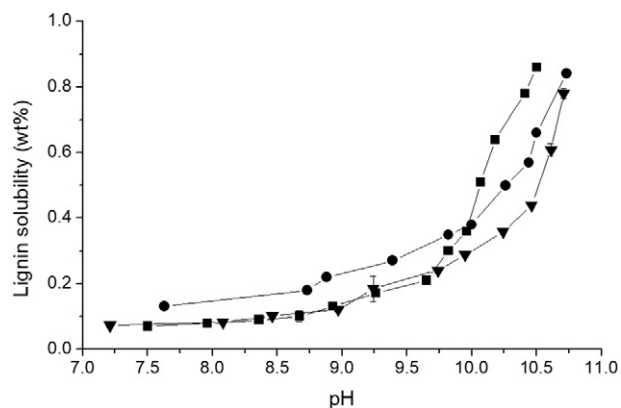


Fig. 5. Solubility of 1 wt% kraft lignin in aqueous LiOH (■), NaOH (●) and KOH (▼) solution as a function of pH at room temperature.

### 3.1.5. Dissolution of kraft lignin in binary systems

Mixtures of different hydroxides have also been considered and generally the higher the fraction of the less efficient hydroxide the worse is the performance of the final solvent mixture. As an example, in Fig. 6, the lignin solubility is plotted for different LiOH/TPAOH weight ratios and it is found to continuously decrease with the increase of the TPAOH fraction.

### 3.2. Characterization of soluble and insoluble fractions of lignin

As discussed above, using 0.1 M NaOH, only ca. 4.3 wt% of lignin is solubilized. Interestingly, the soluble and insoluble fractions are visually different among them and also differ from the starting material (Fig. 7).

#### 3.2.1. Fourier transform infrared spectroscopy and elemental analysis

Apart from the clear visual differences, FTIR analysis was performed on the soluble and insoluble fractions and compared to the initial raw material (Fig. 8). The FTIR spectra were analyzed and the principal band assignments are summarized in Table 2.

In all cases, the FTIR spectra of the initial raw lignin and insoluble fraction are comparable without new peaks. Regardless of the alkaline system used, the main difference found is related to the band intensity. On the other hand, the soluble fraction in NaOH 0.1 M is clearly different, with a drastic increase in the intensity of bands attributed to C—H in-plane deformation of guaiacyl ring, plus secondary alcohols, plus C=O stretch and C—O deformation in secondary alcohols and aliphatic esters. However, in these regions, overlapped vibrations from carbohydrates can also appear revealing the presence polysaccharide impurities [41,42]. The absence of bands at 1750 and 1760  $\text{cm}^{-1}$  suggests that no

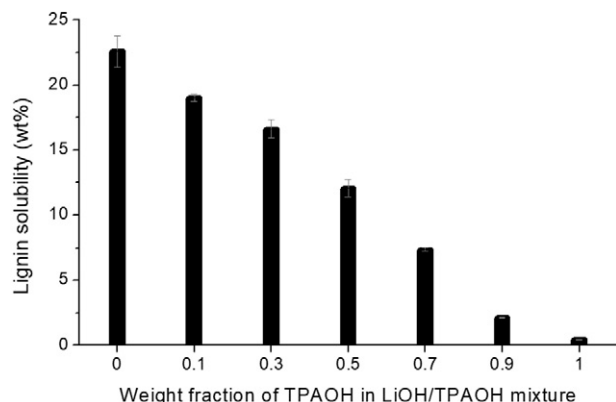


Fig. 6. Solubility of kraft lignin in LiOH/TPAOH mixtures with different ratios.

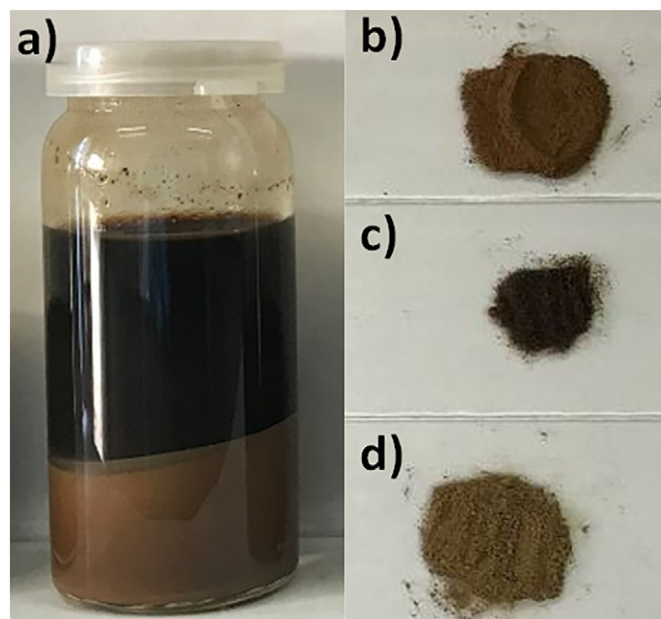


Fig. 7. (a) Macroscopic appearance of 20 wt% kraft lignin dissolved in 0.1 M NaOH after centrifugation and its comparison to the (b) initial lignin and (c) soluble and (d) insoluble lyophilized fractions.

esterification reaction occurred during the dissolution process [43]. Additionally, the intensity of the band attributed to the C—S vibration mode is also enhanced. Note that the initial intensity of the band attributed to the C—S and aromatic skeleton was similar. On the other hand, in the soluble fraction the intensity of C—S band is almost twice the band attributed to the vibration of the aromatic skeleton. This may suggest that this solvent preferably solubilizes lignin fragments enriched with sulfur groups. In order to confirm this hypothesis, elemental analysis was performed, and the relative composition of carbon, hydrogen and sulfur for the raw lignin and soluble and insoluble fractions is reported on Table 3. Indeed, the soluble fraction has a higher content of sulfur in comparison to the raw lignin and insoluble fraction, which agrees with the FTIR data. These results provide support to the idea that the alkaline solvent preferably solubilizes lignin fragments containing sulfur groups due to the favorable intermolecular interactions with the solvent.

#### 3.2.2. Thermogravimetric analysis

The thermal behavior of the soluble and insoluble lignin fractions (after dissolution in 0.1 M NaOH) was determined by thermogravimetric

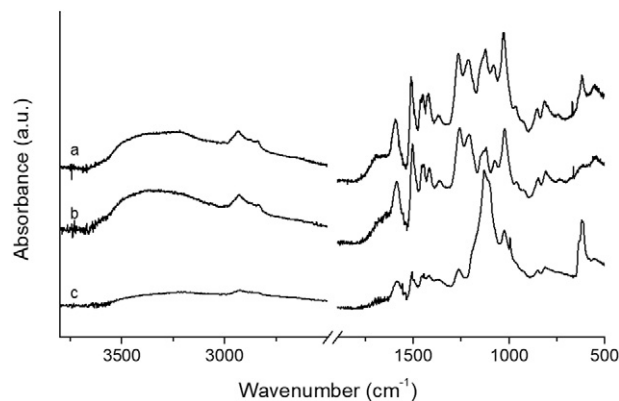


Fig. 8. Normalized FTIR spectra of initial lignin (a) and insoluble (b) and soluble (c) lignin fractions after dissolution in 0.1 M NaOH at room temperature.

**Table 2**  
Band assignments in kraft lignin FTIR spectra.

Wavenumber (cm <sup>-1</sup> )	Assignment
3218	OH stretching in phenolic and aliphatic structures [42,49]
2934	CH stretching in aromatic methoxyl and methylene groups of side chain [42,49]
2838	CH vibration of the -OCH <sub>3</sub> groups [44]
1594	Aromatic skeleton vibration plus C=O stretch [49]
1512	Aromatic skeleton vibration [49]
1460	C-H bending from methyl or methylene groups [44]
1422	Aromatic skeletal vibration combined with CH asymmetric deformation of methyl groups [49]
1367	Phenolic OH and aliphatic C-H in methyl groups [1]
1264	Guaiacyl ring breathing with CO stretch in lignin, CO linkage in guaiacyl aromatic methoxyl groups [44]
1213	C-C plus C-O plus C=O stretch
1123	C-H in-plane deformation of guaiacyl ring plus secondary alcohols plus C=O stretch [49]
1079	C-O deformation in secondary alcohols and aliphatic esters [49]
1028	Aromatic C-H in-plane deformation plus C-O deformation in primary alcohols plus C=O stretch (unconjugated) [49]
854, 814	Aromatic CH out-of-plane bending [44]
617	C-S bonds [44]

**Table 3**  
Elemental composition of initial lignin and soluble and insoluble fraction of 20 wt% kraft lignin dispersed in 0.1 M NaOH.

	%C	%H	%S
Initial lignin	60.71	6.56	1.59
Soluble lignin	50.11	5.73	3.42
Insoluble lignin	61.03	6.57	1.16

analysis (TGA) and compared with the initial raw lignin. Fig. 9 shows the thermal decomposition as well as the corresponding derivative thermogravimetric curves (DTG). The curve evolution can be divided in different steps. In the first step (25–100 °C) lignin dehydration occurs, with the removal of water and other low molecular weight volatiles [1]. The second step can be assigned to the fragmentation of inter-unit linkages, namely the breakage of methyl-aryl ether bonds [1,44,45]. The maximum weight loss in this step appears at 296 °C and 318 °C for soluble and insoluble lignin, respectively, and at 383 °C for the raw lignin. This difference can be related to the different content in C—C linkages [46]. Finally, the last step corresponds to the thermal decomposition and/or condensation of the aromatic rings [1,44,45]. In this step, the soluble lignin is observed to have a distinct weight loss behavior, similar to de-alkaline lignin [47], suggesting that it contains more aromatic compounds. Due to the formation of highly condensed aromatic structures, 26–29 wt% of lignin still

remains unvolatilized even after heating up to 900 °C [46]. This different char residue may be related with the molecular weight since the non-volatile residue is expected to increase with increasing molecular weight [48].

### 3.2.3. Gas chromatography coupled with mass spectroscopy

The TGA data suggests that the soluble lignin fraction has a greater abundance of aromatic compounds. In order to confirm this hypothesis, gas chromatography coupled with mass spectroscopy was performed and a representative spectrum is depicted in Fig. 10. The relative percentage of each compound and possible chemical formula are reported in Table 4.

The soluble fraction has a higher content of compounds with a measured *m/z* of 120.1, which may correspond to an aromatic ring with three branched carbons. This is in agreement with the TGA analysis, where it was found that this fraction contains a greater abundance of aromatic compounds. Compounds with higher molecular weights, namely aromatic rings with larger ramifications and functional groups and dimmers appear for very low intensities and, therefore, have an overall residual contribution.

## 4. Conclusion

In this work a systematic analysis of lignin dissolution in several aqueous-based alkaline solvents was performed for the first time. Most of the alkaline systems tested can dissolve lignin at room temperature. However, their performance varies greatly with the cationic radius; the smaller the cation, the superior the dissolution of lignin. In this context, LiOH is the most efficient system while the hydroxides of bulky cations (e.g. tetralkylammonium) are poor solvents. This behavior is the opposite of other molecules such as cellulose, where such bulky amphiphilic cation plays an important role in dissolution. It is also possible to conclude that increasing the concentration of hydroxide not only improves the amount of lignin dissolved, but also decreases the viscosity of the solution. The Kamlet-Taft parameters  $\pi^*$  and  $\beta$  were evaluated and shown to correlate with the lignin solubility in the alkaline systems, suggesting that these solvatochromic parameters might be good indicators for the screening and development of novel systems. The soluble and insoluble lignin fractions in a selected solvent system (i.e. NaOH) were extensively characterized and data suggests the dissolution of smaller lignin fragments after partial degradation of large lignin molecules. Moreover, data also shows that these alkali-based systems dissolve preferentially lignin molecules enriched with sulfur groups.

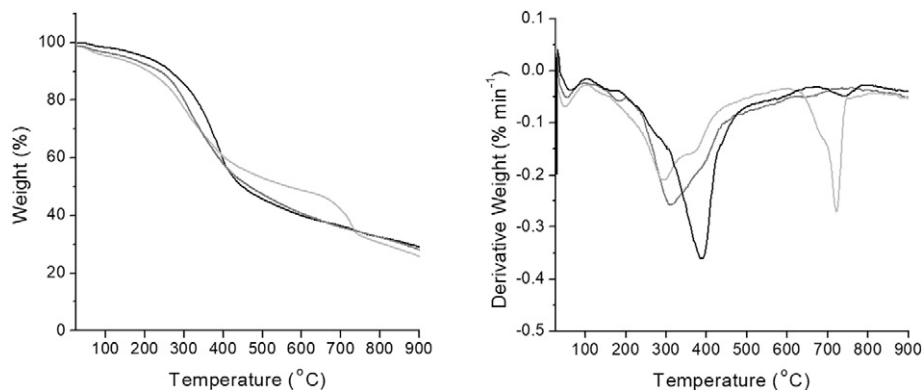


**Fig. 9.** TGA (left) and correspondent DTG (right) of the soluble lignin fraction (light gray line) and insoluble lignin fraction (gray line) after dissolution of 20 wt% kraft lignin in 0.1 M NaOH. The initial raw lignin is represented with a black line.

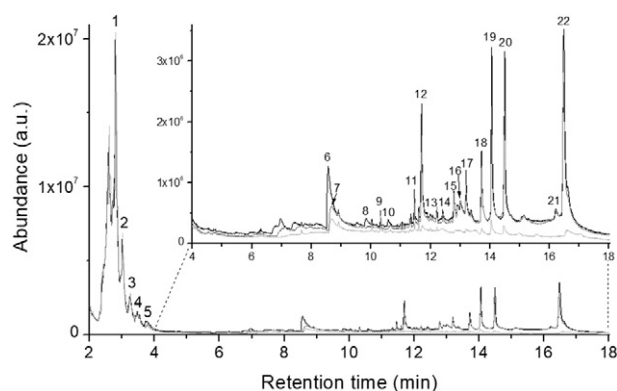


**Fig. 10.** Gas chromatogram of the soluble lignin fraction (light gray line), insoluble lignin fraction (gray line) and initial raw lignin (black line). The different soluble and insoluble fractions were collected after dissolving 20 wt% kraft lignin in 0.1 M NaOH. The assignment of the peaks is represented in table.

Overall, this work highlights and quantifies the performance of different alkaline systems shedding light to the mechanism of dissolution which we consider important for the understanding of the fundamental interactions within a lignin-solvent system, and for

the development of novel processing methodologies which ultimately will help expanding the potential of lignin and its future applications.

#### CRediT authorship contribution statement

**Elodie Melro:** Conceptualization, Investigation, Writing - original draft, Visualization. **Alexandra Filipe:** Investigation, Writing - review & editing. **Dora Sousa:** Writing - review & editing. **Artur J.M. Valente:** Conceptualization, Resources, Writing - review & editing. **Anabela Romano:** Writing - review & editing. **Filipe E. Antunes:** Resources, Writing - review & editing. **Bruno Medronho:** Conceptualization, Writing - review & editing, Supervision, Project administration.

#### Acknowledgements

This work was supported by funding from the Portuguese Foundation for Science and Technology (FCT) through the projects PTDC/AGR-TEC/4814/2014, PTDC/ASP-SIL/30619/2017, UIDB/05183/2020 and the researcher grant IF/01005/2014. Elodie Melro is grateful for the PhD grant (SFRH/BD/132835/2017) from FCT. The CQC is supported by FCT through the project PEstOE/QUI/UI0313/2013.

**Table 4**

List of tentative lignin oligomers detected using GC-MS.

Compound label	Retention time (min)	Measured $m/z$	Chemical formula	% Initial lignin	% Soluble lignin 0.1 M NaOH	% Insoluble lignin 0.1 M NaOH
1	2.8	120.1	C <sub>9</sub> H <sub>12</sub>	63.70	78.97	61.73
2	3.0	134.1	C <sub>10</sub> H <sub>14</sub>	10.15	11.25	11.05
3	3.2	134.1	C <sub>10</sub> H <sub>14</sub>	3.79	4.74	4.41
4	3.5	134.1	C <sub>10</sub> H <sub>14</sub>	2.42	2.37	3.49
5	3.8	148.1	C <sub>11</sub> H <sub>16</sub>	1.48	0.46	1.87
6	8.6	182.1	C <sub>9</sub> H <sub>10</sub> O <sub>4</sub>	2.86	–	–
7	8.7	182.1	C <sub>9</sub> H <sub>10</sub> O <sub>4</sub>	–	0.64	2.13
8	9.8	196.0	C <sub>10</sub> H <sub>12</sub> O <sub>4</sub>	0.26	–	–
9	10.3	270.1	C <sub>13</sub> H <sub>18</sub> O <sub>5</sub>	0.09	0.07	0.11
10	10.6	256.3	C <sub>17</sub> H <sub>20</sub> O <sub>2</sub>	0.15	–	–
11	11.5	254.1	C <sub>16</sub> H <sub>14</sub> O <sub>3</sub>	0.26	0.10	0.28
12	11.7	264.1	C <sub>14</sub> H <sub>16</sub> O <sub>5</sub>	1.32	–	1.89
13	12.2	254.2	C <sub>18</sub> H <sub>22</sub> O	0.07	–	0.23
14	12.4	257	C <sub>15</sub> H <sub>13</sub> O <sub>4</sub>	0.10	–	0.29
15	12.8	274.1	C <sub>16</sub> H <sub>18</sub> O <sub>4</sub>	0.33	–	0.44
16	13.0	274.1	C <sub>16</sub> H <sub>18</sub> O <sub>4</sub>	0.43	–	0.33
17	13.2	303.1	C <sub>16</sub> H <sub>15</sub> O <sub>6</sub>	0.44	–	1.02
18	13.7	304.3	C <sub>17</sub> H <sub>20</sub> O <sub>5</sub>	0.95	–	0.87
19	14.0	300.1	C <sub>17</sub> H <sub>16</sub> O <sub>5</sub>	2.22	0.29	1.73
20	14.5	302.1	C <sub>17</sub> H <sub>18</sub> O <sub>5</sub>	2.41	0.22	1.91
21	16.2	316.1	C <sub>18</sub> H <sub>20</sub> O <sub>5</sub>	0.45	–	0.82
22	16.5	272.1	C <sub>17</sub> H <sub>20</sub> O <sub>3</sub>	5.57	0.50	4.33

## References

- [1] T. Rashid, C.F. Kait, I. Regupathi, T. Murugesan, Dissolution of kraft lignin using protic ionic liquids and characterization, *Ind. Crop. Prod.* (2016) <https://doi.org/10.1016/j.indcrop.2016.02.017>.
- [2] I.F. Fi, F. Peter, C.G. Boeriu, *Structural Analysis of Lignins From Different Sources*, World Acad. Sci. Eng. Technol., 2013.
- [3] J.L. Faulon, P.G. Hatcher, Is there any order in the structure of lignin? *Energy Fuel* (1994) <https://doi.org/10.1021/ef00044a018>.
- [4] J.Y. Kim, E.J. Shin, I.Y. Eom, K. Won, Y.H. Kim, D. Choi, I.G. Choi, J.W. Choi, Structural features of lignin macromolecules extracted with ionic liquid from poplar wood, *Bioresour. Technol.* (2011) <https://doi.org/10.1016/j.biortech.2011.07.081>.
- [5] P. Azadi, O.R. Inderwildi, R. Farnood, D.A. King, Liquid fuels, hydrogen and chemicals from lignin: a critical review, *Renew. Sust. Energ. Rev.* (2013) <https://doi.org/10.1016/j.rser.2012.12.022>.
- [6] L. Zhang, G. Gellerstedt, NMR observation of a new lignin structure, a spiro-dienone, *Chem. Commun.* (2001) <https://doi.org/10.1039/b108285j>.
- [7] A. Toledano, A. García, I. Mondragon, J. Labidi, Lignin separation and fractionation by ultrafiltration, *Sep. Purif. Technol.* (2010) <https://doi.org/10.1016/j.seppur.2009.10.024>.
- [8] N.E. El Mansouri, J. Salvadó, Structural characterization of technical lignins for the production of adhesives: application to lignosulfonate, kraft, soda-anthraquinone, organosolv and ethanol process lignins, *Ind. Crop. Prod.* (2006) <https://doi.org/10.1016/j.indcrop.2005.10.002>.
- [9] J. Hu, Q. Zhang, D.J. Lee, Kraft lignin biorefinery: a perspective, *Bioresour. Technol.* (2018) <https://doi.org/10.1016/j.biortech.2017.08.169>.
- [10] Y. Kim, J. Suhr, H. Seo, H. Sun, S. Kim, I. Park, S.-H. Kim, Y. Lee, K. Kim, J. Nam, All biomass and UV protective composite composed of compatibilized lignin and poly (lactic-acid), *Sci. Rep.* 7 (2018) 1–11, <https://doi.org/10.1038/srep43596>.
- [11] Y. Ren, X. Qiu, J. Wang, Y. Qian, D. Yang, Y. Deng, Reduction of lignin color via one-step UV irradiation, *Green Chem.* 18 (2016) 695–699, <https://doi.org/10.1039/c5gc02180d>.
- [12] M. Pishnamazi, H.Y. Ismail, S. Shirazian, J. Iqbal, G.M. Walker, M.N. Collins, Application of lignin in controlled release: development of predictive model based on artificial neural network for API release, *Cellulose* (2019) <https://doi.org/10.1007/s10570-019-02522-w>.
- [13] M. Pishnamazi, H. Hafizi, S. Shirazian, M. Culebras, G.M. Walker, M.N. Collins, Design of controlled release system for paracetamol based on modified lignin, *Polymers* (Basel, Switz.) (2019) <https://doi.org/10.3390/POLYM11061059>.
- [14] A. Beaucamp, Y. Wang, M. Culebras, M.N. Collins, Carbon fibres from renewable resources: the role of the lignin molecular structure in its blendability with biobased poly(ethylene terephthalate), *Green Chem.* (2019) <https://doi.org/10.1039/c9gc02041a>.
- [15] M. Culebras, M.J. Sanchis, A. Beaucamp, M. Carsí, B.K. Kandola, A.R. Horrocks, G. Panzetti, C. Birkinshaw, M.N. Collins, Understanding the thermal and dielectric response of organosolv and modified kraft lignin as a carbon fibre precursor, *Green Chem.* (2018) <https://doi.org/10.1039/c8gc01577e>.
- [16] S. Laurichesse, L. Avérous, Chemical modification of lignins: towards biobased polymers, *Prog. Polym. Sci.* 39 (2014) 1266–1290, <https://doi.org/10.1016/j.procpolymsci.2013.11.004>.
- [17] A. Vishtal, A. Kraslawski, Challenges in industrial applications of technical lignins, *BioResources* (2011) <https://doi.org/10.15376/BIORES.6.3.3547-3568>.
- [18] J. Zakzeski, P.C.A. Bruijninx, A.L. Jongerius, B.M. Weckhuysen, The catalytic valorization of lignin for the production of renewable chemicals, *Chem. Rev.* (2010) <https://doi.org/10.1021/cr900354u>.
- [19] F.G. Calvo-Flores, J.A. Dobado, Lignin as renewable raw material, *ChemSusChem* (2010) <https://doi.org/10.1002/cssc.201000157>.
- [20] M. Lake, C. Scouten, What are we going to do with all this lignin, *Front. BioRefining Conf.* 2014.
- [21] S. Beisl, A. Miltner, A. Friedl, Lignin from micro- to nanosize: production methods, *Int. J. Mol. Sci.* 18 (2017) <https://doi.org/10.3390/ijms18061244>.
- [22] E. Melro, L. Alves, F.E. Antunes, B. Medronho, A brief overview on lignin dissolution, *J. Mol. Liq.* 265 (2018) <https://doi.org/10.1016/j.molliq.2018.06.021>.
- [23] T.J. Szalaty, Ł. Klapiszewski, M. Stanis, D. Moszyński, A. Skrzypczak, T. Jesionowski, Catalyst-free activation of kraft lignin in air using hydrogen sulfate ionic liquids, *Int. J. Biol. Macromol.* (2018) <https://doi.org/10.1016/j.ijbiomac.2018.07.152>.
- [24] Ł. Klapiszewski, T.J. Szalaty, B. Kurc, M. Stanis, B. Zawadzki, A. Skrzypczak, T. Jesionowski, Development of acidic imidazolium ionic liquids for activation of kraft lignin by controlled oxidation: comprehensive evaluation and practical utility, *Chempluschem* (2018) <https://doi.org/10.1002/cplu.201800123>.
- [25] T.J. Szalaty, Ł. Klapiszewski, B. Kurc, A. Skrzypczak, T. Jesionowski, A comparison of protic and aprotic ionic liquids as effective activating agents of kraft lignin. Developing functional MnO<sub>2</sub>/lignin hybrid materials, *J. Mol. Liq.* (2018) <https://doi.org/10.1016/j.molliq.2018.04.044>.
- [26] S. Sarkanen, D.C. Teller, C.R. Stevens, J.L. McCarthy, Lignin. 20. Associative interactions between kraft lignin components, *Macromolecules* (1984) <https://doi.org/10.1021/ma00142a022>.
- [27] M.K.R. Konduri, P. Fatehi, Production of water-soluble hardwood kraft lignin via sulfomethylation using formaldehyde and sodium sulfite, *ACS Sustain. Chem. Eng.* (2015) <https://doi.org/10.1021/acssuschemeng.5b00098>.
- [28] E.I. Evstigneev, Specific features of lignin dissolution in aqueous and aqueous-organic media, *Russ. J. Appl. Chem.* (2010) <https://doi.org/10.1134/s1070427210030250>.
- [29] S. Sarkanen, S. Sarkanen, D.C. Teller, E. Abramowski, J.L. McCarthy, Lignin. 19. Kraft lignin component conformation and associated complex configuration in aqueous alkaline solution, *Macromolecules* (1982) <https://doi.org/10.1021/ma00232a027>.
- [30] D.J. Eyckens, B. Demir, T.R. Walsh, T. Welton, L.C. Henderson, Determination of Kamlet-Taft parameters for selected solvate ionic liquids, *Phys. Chem. Chem. Phys.* (2016) <https://doi.org/10.1039/c6cp01216g>.
- [31] M.J. Kamlet, J.L. Abboud, R.W. Taft, The solvatochromic comparison method. 6. The  $\pi^*$  scale of solvent polarities.1, *J. Am. Chem. Soc.* (1977) <https://doi.org/10.1021/ja00460a031>.
- [32] D. González-Arjona, G. López-Pérez, M.M. Domínguez, A.G. González, Solvatochromism: a comprehensive project for the final year undergraduate chemistry laboratory, *J. Lab. Chem. Educ.* (2016) <https://doi.org/10.5923/j.ljce.20160403.01>.
- [33] P. Gong, J. Wang, B. Liu, G. Ru, J. Feng, Dissolution of chitin in aqueous KOH, *Cellulose* (2016) <https://doi.org/10.1007/s10570-016-0932-z>.
- [34] B. Medronho, H. Duarte, L. Alves, F.E. Antunes, A. Romano, A.J.M. Valente, The role of cyclodextrin-tetrabutylammonium complexation on the cellulose dissolution, *Carbohydr. Polym.* (2016) <https://doi.org/10.1016/j.carbpol.2015.12.026>.
- [35] Y.N. Kuo, J. Hong, Investigation of solubility of microcrystalline cellulose in aqueous NaOH, *Polym. Adv. Technol.* (2005) <https://doi.org/10.1002/pat.595>.
- [36] M.M. Elsemongy, A.A. Abdel-Khalek, Ionic radii in aqueous solutions, *J. Electrochem. Soc. India* 38 (1989) 163–173.
- [37] R. Rinaldi, Instantaneous dissolution of cellulose in organic electrolyte solutions, *Chem. Commun.* (2011) <https://doi.org/10.1039/c0cc02421j>.
- [38] A. Samanta, A. Bera, K. Ojha, A. Mandal, Effects of alkali, salts, and surfactant on rheological behavior of partially hydrolyzed polyacrylamide solutions, *J. Chem. Eng. Data* (2010) <https://doi.org/10.1021/je100458a>.
- [39] S.I. Mussatto, M. Fernandes, I.C. Roberto, Lignin recovery from brewer's spent grain black liquor, *Carbohydr. Polym.* (2007) <https://doi.org/10.1016/j.carbpol.2007.03.021>.
- [40] Z. Wei, Y. Yang, R. Yang, C. Wang, Alkaline lignin extracted from furfural residues for pH-responsive Pickering emulsions and their recyclable polymerization, *Green Chem.* (2012) <https://doi.org/10.1039/c2gc36278c>.
- [41] C. Mattsson, M. Hasani, B. Dang, M. Mayzel, H. Theliander, About structural changes of lignin during kraft cooking and the kinetics of delignification, *Holzforchung* (2017) <https://doi.org/10.1515/hf-2016-0190>.
- [42] C.G. Boeriu, D. Bravo, R.J.A. Gosselink, J.E.G. Van Dam, Characterisation of structure-dependent functional properties of lignin with infrared spectroscopy, *Ind. Crop. Prod.* 20 (2004) 205–218, <https://doi.org/10.1016/j.indcrop.2004.04.022>.
- [43] J. Lisperguer, P. Perez, S. Urizar, Structure and thermal properties of lignins: characterization by infrared spectroscopy and differential scanning calorimetry, *J. Chil. Chem. Soc.* 54 (2009) 460–463, <https://doi.org/10.4067/S0717-97072009000400030>.
- [44] S. Sathawong, W. Sridach, K.A. Techato, Lignin: isolation and preparing the lignin based hydrogel, *J. Environ. Chem. Eng.* (2018) <https://doi.org/10.1016/j.jece.2018.05.008>.
- [45] R.C. Sun, J. Tomkinson, G. Lloyd Jones, Fractional characterization of ash-AQ lignin by successive extraction with organic solvents from oil palm EFB fibre, *Polym. Degrad. Stab.* (2000) [https://doi.org/10.1016/S0141-3910\(99\)00174-3](https://doi.org/10.1016/S0141-3910(99)00174-3).
- [46] A. Tejado, C. Peña, J. Labidi, J.M. Echeverría, I. Mondragon, Physico-chemical characterization of lignins from different sources for use in phenol-formaldehyde resin synthesis, *Bioresour. Technol.* (2007) <https://doi.org/10.1016/j.biortech.2006.05.042>.
- [47] Q. Wang, D. Tian, J. Hu, F. Shen, G. Yang, Y. Zhang, S. Deng, J. Zhang, Y. Zeng, Y. Hu, Fates of hemicellulose, lignin and cellulose in concentrated phosphoric acid with hydrogen peroxide (PHP) pretreatment, *RSC Adv.* (2018) <https://doi.org/10.1039/c8ra00764k>.
- [48] T.-Q. Yuan, F. Xu, S.-N. Sun, R.-C. Sun, M.-F. Li, Effect of ionic liquid/organic solvent pretreatment on the enzymatic hydrolysis of corn cob for bioethanol production. Part 1: structural characterization of the lignins, *Ind. Crop. Prod.* 43 (2012) 570–577, <https://doi.org/10.1016/j.indcrop.2012.07.074>.
- [49] O. Faix, Classification of lignins from different botanical origins by FT-IR spectroscopy, *Holzforchung* (1991) <https://doi.org/10.1515/hfsg.1991.45.s1.21>.